

## Charge-density distribution of Be metal studied by $\gamma$ -ray diffractometry

Niels Kristian Hansen\* and Jochen R. Schneider

*Hahn-Meitner-Institut für Kernforschung, Glienicker Strasse 100, D-1000 Berlin 39, Federal Republic of Germany*

Finn Krebs Larsen

*Department of Chemistry Aarhus University, DK-8000 Aarhus C, Denmark*

(Received 7 December 1982; revised manuscript received 25 May 1983)

With a  $\gamma$ -ray diffractometer, eight extinction-free structure factors for beryllium have been measured on an absolute scale with an accuracy of about 0.5%. These data are in good agreement with another recent measurement by Larsen and Hansen using x rays, but in serious disagreement with an earlier set of x-ray data due to Brown. The  $\gamma$ -ray structure factors are compared with results of SCF-HF-LCAO (self-consistent-field, Hartree-Fock, linear combination of atomic orbitals) and APW (augmented-plane-wave) band-structure calculations. Theoretical and experimental structure factors are in reasonable agreement except for the two lowest-order reflections. A significant improvement of the APW results may be obtained by going beyond the muffin-tin approximation. Renormalized-free-atom and OPW (orthogonalized-plane-wave) model calculations show that the structure factors are sensitive to the average form of the wave functions, whereas Compton profiles mainly depend on the orthogonality of the wave functions.

### I. INTRODUCTION

The present  $\gamma$ -ray diffraction measurements on beryllium were inspired by the standard x-ray diffraction measurements by Larsen and Hansen,<sup>1</sup> the earlier neutron-diffraction study by Larsen, Lehmann, and Merisalo,<sup>2</sup> the Compton scattering and absolute x-ray structure-factor measurements by Manninen and Suortti,<sup>3</sup> and the Compton scattering experiments by Hansen, Pattison, and Schneider.<sup>4</sup>

The x-ray data by Larsen and Hansen,<sup>1</sup> when scaled on high-order reflections by means of least-squares refinement techniques, show a discrepancy with an earlier set of x-ray data, measured on an absolute scale by Brown.<sup>5</sup> The purpose of the  $\gamma$ -ray measurements was to obtain accurate, extinction-free structure factors on an absolute scale for a few of the low-order reflections ( $\sin\theta/\lambda \leq 0.5 \text{ \AA}^{-1}$ ) with the intention of using these structure factors to check the scale of the relative x-ray measurements by Larsen and Hansen.

Suortti<sup>6</sup> measured the three lowest-order reflections for beryllium on an absolute scale using molybdenum and copper  $K\alpha$  radiation. By comparing the measured reflectivities for different wavelengths, and for different polarizations of the incident beam, the integrated intensities were corrected for effects of both secondary and primary extinction. His results were also very different from those obtained by Brown.

Larsen and Hansen<sup>1</sup> calculated the charge-density distribution in beryllium from their x-ray diffraction data and did not find marked evidence of anisotropy in the bonding. This result is in disagreement with the conclusion drawn by Brown in the discussion of her data, as well as with the findings of Stewart<sup>7</sup> and Yang and Coppens<sup>8</sup> from their interpretation of Brown's data. The valence densities derived from Brown's data were almost

identical to the results of an augmented-plane-wave (APW) calculation on beryllium.<sup>9</sup> A recent APW calculation by Redinger, Bauer, and Hansen<sup>10</sup> shows the same features in the electron density distribution as the earlier calculation, but this time x-ray structure factors have also been obtained from the wave functions.

Recently, Dovesi, Pisani, Ricca, and Roetti,<sup>11</sup> using a crystal linear combination of atomic orbitals Hartree-Fock (LCAO-HF) method, have calculated band structure, form factors, and Compton profiles for beryllium metal. They do find that  $p$ -like states are important in the bonding, but they do not find a prevalence of one  $p$  orbital over another from their calculations.

In the following, we shall center our discussion on the form factors of beryllium obtained in the  $\gamma$ -ray experiment. In Sec. II, we give a short description of the experiment in general and present measurements on imperfect silicon samples which we use as a test of the reliability of our experimental method. The actual measurements on beryllium single crystals are described in Sec. III, and the present results are compared with other experimental work in Sec. IV. As with the structure factors, Compton profile measurements using high-energy  $\gamma$  radiation only depend on the ground-state wave functions, and we therefore compare both experimental structure factors and previous Compton profile measurements with the theoretical predictions by Dovesi *et al.*<sup>11</sup> In order to get a better understanding of the origin of the gross features in the observed quantities, we have, furthermore, calculated both structure factors and Compton profiles from simple crystal wave-function models (Sec. V).

### II. EXPERIMENTAL

The structure-factor measurements were carried out on the four-circle  $\gamma$ -ray diffractometer at the Hahn-Meitner-

Institut, described by Schneider, Pattison, and Graf.<sup>12</sup> A neutron-activated gold source delivers  $\gamma$  radiation with a wavelength of 0.0301 Å and with an energy resolution  $\Delta\lambda/\lambda=10^{-6}$ . The angular resolution for an incident beam of 2 mm diam equals  $\Delta\omega=2.64'$ . All reflections are measured in symmetrical Laue geometry, and both the diffracted and transmitted intensities are measured in order to obtain the integrated reflectivities on an absolute scale. The Bragg reflections are step-scanned in the  $\omega$  mode. The intrinsic germanium detector of the diffractometer allows excellent energy discrimination, and in consequence the background in the measurements is very low (0.1–0.01 counts/s, depending on the scattering angle). In this work, the transmitted intensity is measured before and after each set of scans of a reflection, and each time with the setting of the crystal corresponding to the beginning and the end point of the scan, i.e., well away from the Bragg position.

The measured intensities were corrected for coincidence loss, which mainly affects the transmitted beam intensity. The dead time of the counting chain was determined to 6.9  $\mu$ s with a standard deviation of 0.4  $\mu$ s using the method of Chipman.<sup>13</sup> The intensity of the incident beam is of the order of  $4 \times 10^3$  counts/s, resulting in coincidence loss corrections of 2–3%. In the measurements reported here, the peak reflectivity was always less than 0.2% resulting in a maximum peak count rate of the order of 5 counts/s. Therefore, counting statistics is the main limiting factor for the accuracy of the  $\gamma$ -ray structure-factor measurements on beryllium.

For an ideally imperfect single crystal, the integrated reflectivity  $R_{\text{kin}}$  is related to the structure factor  $F$  (neglecting thermal diffuse scattering) as follows:

$$R_{\text{kin}} = QT_0 / \cos\theta_B,$$

with

$$Q = \left[ \frac{r_0 \lambda F}{V} \right]^2 \frac{\lambda}{\sin(2\theta_B)} P(\theta_B), \quad (1)$$

where  $r_0$  is the classical electron radius,  $\lambda$  represents the wavelength,  $V$  the unit-cell volume, and  $T_0$  the crystal thickness.  $\theta_B$  is the Bragg angle, and

$$P(\theta_B) = \frac{1}{2} [1 + \cos^2(2\theta_B)]$$

is the polarization factor.

The importance of a possible correction of the measured Bragg intensities for secondary extinction can be estimated on the basis of Darwin's extinction theory.<sup>14</sup> For symmetrical Laue geometry and a Gaussian mosaic distribution function, the measured integrated reflecting power  $R_m$  can be expressed as

$$R_m = R_{\text{kin}} e^{-gR_{\text{kin}}}, \quad g = (2 \ln 2 / \pi)^{1/2} / \omega_M, \quad (2)$$

where  $\omega_M$  is the full width at half maximum (FWHM) of the mosaic distribution which can be measured by  $\gamma$ -ray diffractometry whenever  $\omega_M$  is larger than the angular resolution of the diffractometer. In the present case it turns out that the effect of the reduction of the measured integrated reflecting power due to secondary extinction on the experimental structure factors is always much smaller

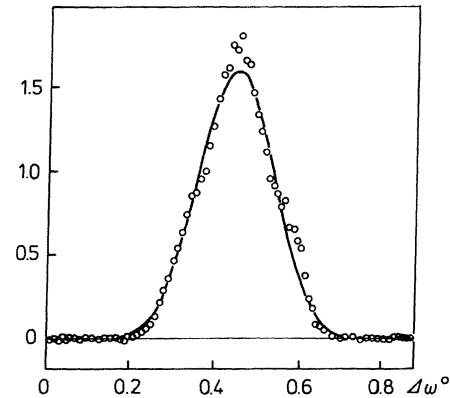


FIG. 1. Silicon rocking curve for (111) reflection. Vertical scale gives the reflectivity in units of 0.1%. Solid curve shows a Gaussian fit to the observed reflectivity curve.

than the statistical error of our experiment.

In order to check the reliability of the structure factors obtained using our  $\gamma$ -ray diffractometer, we measured two reflections on imperfect silicon crystals prepared by A. Freund at the Institut Laue Langevin (ILL), Grenoble. The experimental structure factors are then compared with the very accurate results obtained by Aldred and Hart<sup>15</sup> on perfect Si single crystals using the Pendellösung method. In Fig. 1 we show one of the measured  $\gamma$  rocking curves. We only measured the two lowest-order reflections, i.e., (111) and (220), in order to make sure that thermal diffuse scattering constitutes an insignificant part of the diffracted intensity.

Table I shows the mean structure-factor values obtained from two series of measurements. Each reflection was measured for four different settings. Between the  $\omega$  scans, the crystal was turned 0.5° around the scattering vector. In agreement with earlier estimations<sup>16</sup> we do not find any evidence that our measurements are biased by multiple Bragg scattering.

The major contribution to the random error on the results comes from the determination of the crystal thickness which was measured with a micrometer screw gauge. The miscut of the crystal is determined on the diffractometer looking at the reflection from a polished surface of the sample of a laser beam which is parallel to the  $\gamma$ -ray beam. Because of the low scattering angles ( $\theta_B \leq 0.5^\circ$ ),

TABLE I. Silicon structure factors.

$h$	$k$	$l$	$F(\text{AH})^a$	$F(\gamma)^b$
1	1	1	60.04(3) <sup>c</sup>	60.02(18) <sup>c</sup>
2	2	0	67.08(7) <sup>c</sup>	67.15(20) <sup>c</sup>

<sup>a</sup> $F(\text{AH})$  from Aldred and Hart (Ref. 15).

<sup>b</sup> $F(\gamma)$  from present study.

<sup>c</sup>The estimated standard deviations in parentheses are for the  $\gamma$ -ray data mainly due to the uncertainty in the measurement of the crystal thickness.

the miscut may be taken into account by modifying the thickness  $T_0$  in Eq. (1).

In Fig. 2, the resulting structure factors are compared with the values obtained by Aldred and Hart (Ref. 15, Table 2) on perfect silicon crystals, the effect of thermal vibration was included using the Debye-Waller factor  $B=0.4613 \text{ \AA}^2$  determined by Aldred and Hart. The agreement is found to be excellent with the Aldred and Hart values falling well within one standard deviation of the average values of the  $\gamma$  structure factors. Since we used the identical procedure for the collection of the beryllium data, we consider this an indication of the accuracy of the data presented in the following.

### III. BERYLLIUM STRUCTURE-FACTOR MEASUREMENTS

Beryllium single crystals were grown at and kindly supplied by the Max-Planck-Institut für Metallforschung, Stuttgart. Two plane-parallel plates had been cut with spark erosion. One had its faces perpendicular to (100) and was 2.58 mm thick, the other one was cut perpendicular to (110) with a thickness of 2.94 mm. The (100) crystal had been etched so that it was about 0.2 mm thinner than cut in order to ensure that the intensities were not affected by poor surface quality. Inspection of the crystal under a microscope showed only a very slight unevenness of the surface, certainly less than the error of measurement of the thickness which is of the order of 0.01 mm. A comparison of the intensities for the (002) and (004) reflections which could be measured on both samples indicated that the error in the thickness determination was smaller than 0.5%.

Each reflection has been measured in different volume elements of the sample and possible bias of the intensities

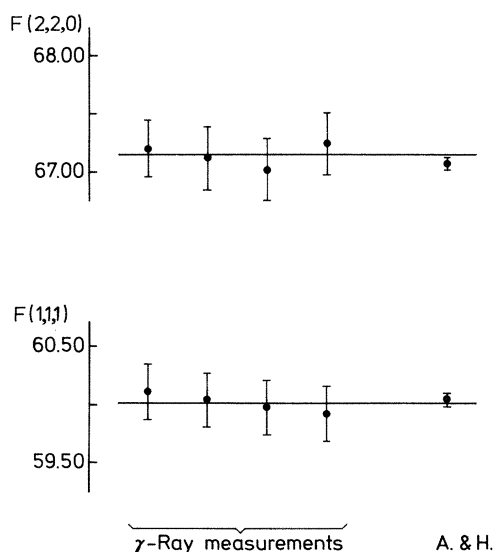


FIG. 2. Comparison of the single measured factors with the results of Aldred and Hart (Ref. 15) denoted A & H. Error bars show plus or minus one standard deviation. Horizontal lines represent the average value of the  $\gamma$ -ray measurements.

due to multiple scattering was checked by rotating the sample around the scattering vector. The resulting structure factors are given in Table II. The rocking curves appeared as single or double peaks. The peak widths are about  $3'$ . Taking into account the angular resolution ( $\text{FWHM}=2.64'$ ), the width of the mosaic distributions is of the order of  $1'$ . The maximum observed peak reflectivity was 0.17% [for the (002) reflection] which for the intrinsic diffraction pattern corresponds to a peak reflectivity of about 0.5–1.0%. We therefore expect secondary extinction to be small. Using Darwin's extinction theory for the (002) reflection, we calculate an extinction factor,  $\gamma=0.994$ . In Fig. 3 we show four rocking curves for different volume elements of two crystals. Curves (a)–(c) are measured on one crystal and (d) on the other. The values obtained for the structure factor  $F(002)$ , are 3.35, 3.32, 3.32, and, 3.31, respectively, with estimated random errors of 0.02. The good agreement between these four measurements is another indication that extinction is of minor importance for our data.

### IV. COMPARISON OF EXPERIMENTALLY DETERMINED STRUCTURE FACTORS

In the Introduction we gave a list of previous experiments. In Fig. 4 we have shown the deviation of the structure factors measured by Brown,<sup>5</sup> Suortti,<sup>6</sup> and the present  $\gamma$ -ray data from those by Larsen and Hansen.<sup>1</sup> Brown's data are on the average 7% lower than Larsen's and with as high a deviation as 11% for the (002) reflection, which is of the strongest reflection. The  $\gamma$ -ray results do not deviate significantly from Larsen and Hansen's x-ray values. The agreement between the present data and Suortti's is good, except for the lowest-order reflection. The random errors of Suortti's data are close to 1%. Since there is no overlap of the  $\gamma$ -ray data set and the x-ray data set by Manninen and Suortti<sup>3</sup> we refrain from discussing their results.

Based on the results of the present work, one is led to suspect that Brown's data are not free from extinction as she assumed. These data were measured in equatorial transmission geometry and so Eqs. (1) and (2) also apply to that experiment. In order to test Brown's hypothesis of insignificant extinction we have plotted  $\ln(F_{\text{Brown}}/F_{\gamma})$  as a function of  $QT_0/2\cos\theta_B$  for the reflections which Brown measured on an absolute scale (Fig. 5).  $Q$  is calculated using the  $\gamma$ -ray structure factors. This plot should

TABLE II. Beryllium structure factors from present study.

$h$	$k$	$l$	$F(\text{standard deviation})$
0	0	2	3.320(7)
0	0	4	2.196(10)
1	0	0	1.833(6)
1	0	1	2.828(7)
1	0	2	1.455(11)
1	0	3	2.168(12)
2	0	0	1.214(7)
1	1	0	2.659(18)

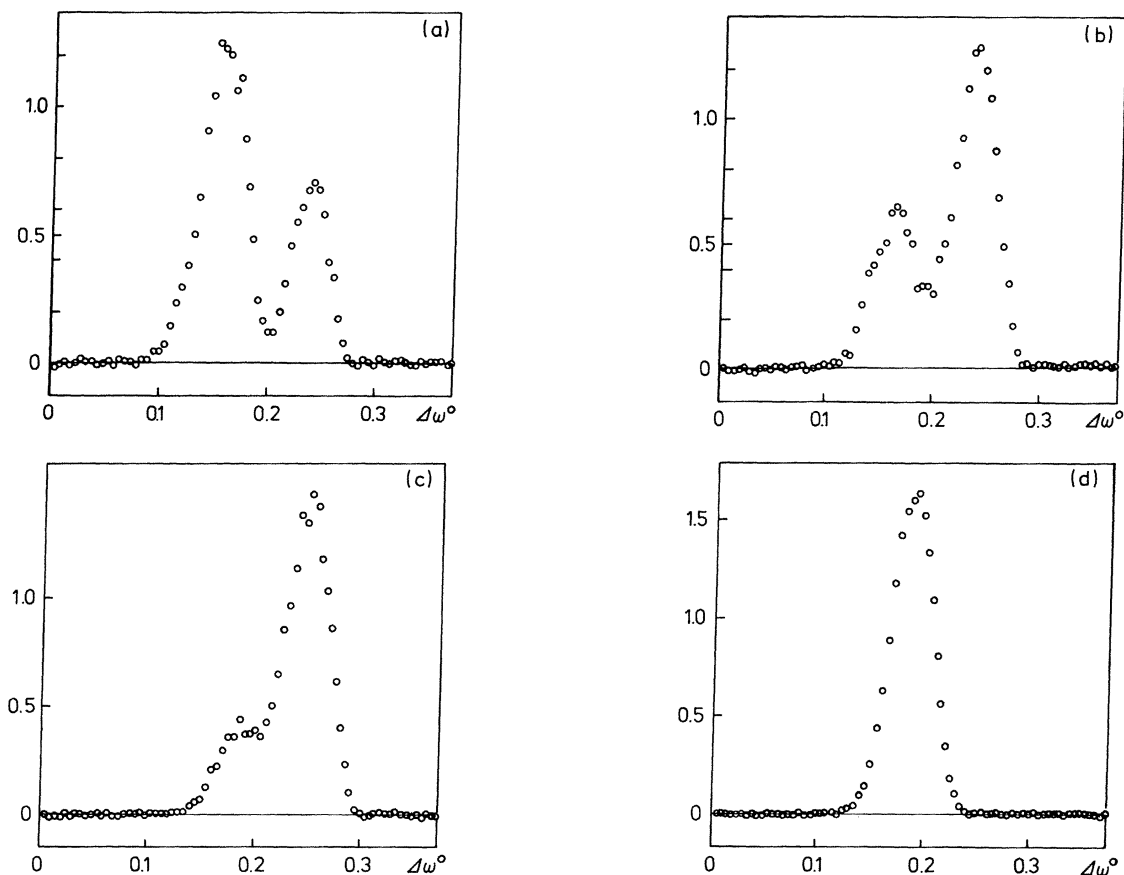


FIG. 3. Beryllium rocking curves for the (002) reflection from different parts of the samples. Vertical scale gives the reflectivity in units of 0.1%.

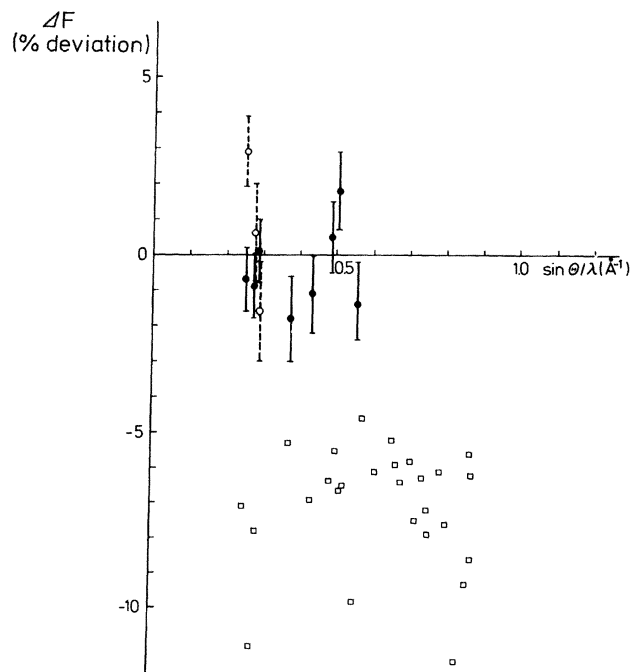


FIG. 4. Deviation from the x-ray structure factors measured by Larsen and Hansen (Ref. 1) of the measurements by Suortti (Ref. 6),  $\circ$ ; by P. J. Brown (Ref. 5),  $\square$ ; and in the present experiment,  $\bullet$ . Error bars show plus or minus one standard deviation.

result in a straight line of zero slope if extinction is negligible, since the following relation should hold under the assumption of homogeneous isotropic Gaussian mosaic distribution:

$$\ln(F_{\text{Brown}}/F_{\gamma}) = \ln(\text{scale}) - \frac{1}{2}gQT_0/\cos\theta_B.$$

"Scale" denotes a possible scale-factor error in either the  $\gamma$ - or the x-ray data set.

For both of Brown's crystals we observe a reasonable fit with such a functional form (Fig. 5). For one of the samples, we conclude that extinction is unimportant, but that the scale factor is in error. For the other extinction is serious and there is no significant scaling error. The predicted mosaic spread is, in the latter case,  $\omega_M = 3' \pm 1'$ . Because of all the assumptions involved in the above analysis, we can only take it as an indication that extinction may be serious in Brown's data. This observation is in line with the work by Suortti<sup>6</sup> who finds that primary as well as secondary extinction is likely to play an important role for x-ray measurements on beryllium samples of the thickness used in Brown's experiment. It should be noted that mean-square amplitudes of thermal vibration deduced from Brown's x-ray data far exceed values calculated on the basis of later diffraction studies which all give values in good agreement with the results of the short-wavelength neutron-diffraction study of Larsen *et al.*<sup>2</sup> In view of the serious doubts cast on Brown's x-ray structure

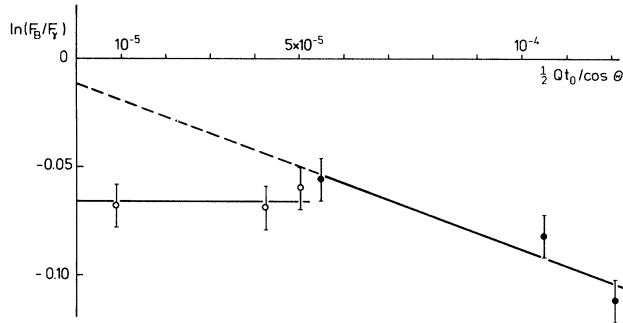


FIG. 5. Behavior of  $\ln(F_B/F_\gamma)$ , where  $F_B$  is the (Ref. 5) absolute structure factor measured by Brown (Ref. 5) and  $F_\gamma$  is the structure factor from the present study. ● corresponds to measurements by Brown on a crystal slab cut perpendicular to [110], and ○ corresponds to those cut perpendicular to [001].

factors concerning scale and extinction we will in the following analysis concentrate our attention on the more recent sets of structure factors.

The crystal structure of beryllium at room temperature is hexagonal-closed packed with two atoms in the unit cell in positions with coordinates  $\pm(\frac{1}{3}, \frac{2}{3}, \frac{1}{4})$ . The structure factors  $F(hkl)$  can be described by the expression

$$F(h,k,l) = 2f \left[ \frac{\sin\theta}{\lambda} \right] \cos 2\pi \left[ \frac{h-k}{3} + \frac{l}{4} \right] T(h,k,l),$$

which then defines the experimental atomic form factor  $f$ . The Debye-Waller factor  $T(h,k,l)$  is calculated using the vibrational amplitudes obtained in the neutron-diffraction analysis by Larsen *et al.*<sup>2</sup> Since we are only looking at

low-order reflections, the uncertainty in the thermal parameters due to thermal diffuse scattering are relatively unimportant compared with the experimental errors in the x-ray and  $\gamma$ -ray experiments. We may then compare the "crystal form factor" with the form factor for the free atom, and here we shall use the HF form factors.<sup>17</sup> The differences between these and form factors from correlated wave functions<sup>18</sup> are small for  $\sin\theta/\lambda \geq 0.25 \text{ \AA}^{-1}$ , which is at the attainable region of momentum transfer in the crystal.

The present experiment shows only small deviations from a free-atom model (Fig. 6). The most pronounced disagreement is for the (100) reflection which we find to be significantly stronger than predicted by the free-atom form factor ( $f - f_{\text{atom}} = [0.07(1)]e$ ). Larsen and Hansen's x-ray form factors show similar deviations as the  $\gamma$ -ray form factor from the free-atom values. The form factors corresponding to the three low-order structure factors measured by Suortti also deviate in the same manner from the free-atom form factor, and actually the deviation for the (100) structure factor is even more pronounced (see Fig. 6).

#### V. COMPARISON OF EXPERIMENTAL FORM FACTORS AND COMPTON PROFILES WITH THEORETICAL CALCULATIONS

Dovesi *et al.*<sup>11</sup> have calculated both band structure, structure factors, and Compton profiles for beryllium. In Fig. 7 their form-factor results are shown as deviations from the free-atom form factor. In the same figure we once again show the deviation of the  $\gamma$ -ray form factors from the free-atom form factor.

The largest disagreement between this theory and the present experimental form factors is found for (010), the

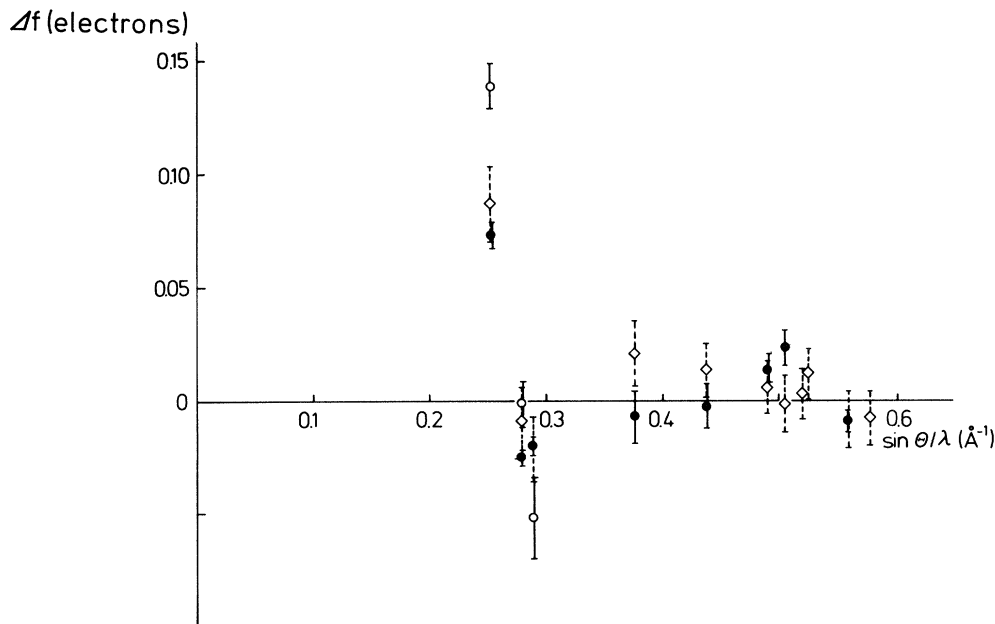


FIG. 6. Deviation of experimental form factors from the free-atom HF form factor (Ref. 17) as follows: Suortti (Ref. 6), ○; Larsen and Hansen (Ref. 1), ◇; and present experiment, ●.

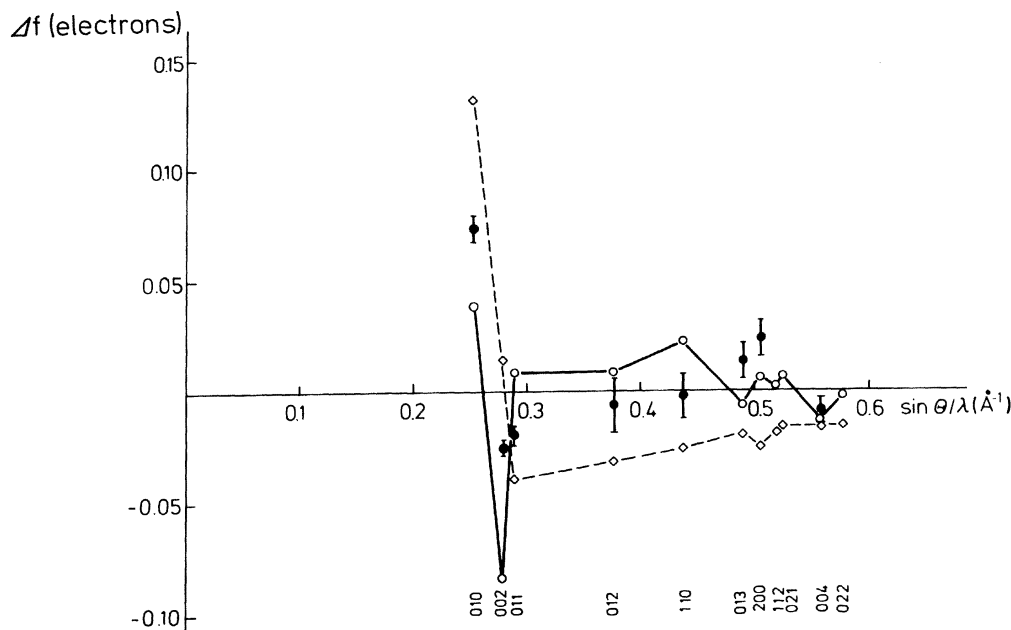


FIG. 7. Deviation of the theoretical form factors from the free-atom HF form factor as follows: HF LCAO of Dovesi *et al.* (Ref. 11),  $\diamond$ ; and APW of Redinger *et al.* (Ref. 10),  $\circ$ . Also shown are the present experimental values,  $\bullet$ .

lowest-order reflection, but the trend relative to the free atom is the same, both having higher values. For the (002) reflection the theoretical value is a little above and the experimental a little below the free atom, whereas the agreement is quite close for the third reflection, (011). The experimental deviations for the following reflections up to  $\sin\theta/\lambda=0.5 \text{ \AA}^{-1}$  tend to lie above the curve of Dovesi *et al.*, and the experimental values are in closer agreement with the free-atom model than the results by Dovesi *et al.* are.

In Fig. 7 we also show the results of the APW calculation by Redinger *et al.*<sup>10</sup> It is seen to be in about as close an agreement with the present experiment as the HF calculation. For the lowest-order reflections the experimental form factors fall halfway between the theoretical ones.

In the following we shall present calculations of form factors and Compton profiles from simple models in an attempt to find the origin of the gross features that we have observed. The model wave functions obey the translational crystal symmetry and take into account the orthogonality of the valence and/or conduction electrons to the atomic cores.

We have already noted that the measured form factors were close to the free-atom form factors, whereas the experimental Compton profiles certainly show considerable deviations from the free atom and are much closer to a free-electron gas. In order to solve this "paradox" we constructed two sets of crystal functions.

We shall first examine a set of single orthogonalized-plane-wave (OPW) functions, i.e., the crystal wave functions are

$$\chi_{\vec{k}}(\vec{r}) = e^{i\vec{k}\cdot\vec{r}} + a_{\vec{k}}\chi_{\vec{k}}^{\text{core}}(r),$$

where  $\chi_{\vec{k}}^{\text{core}}$  is the tightly bound core wave function for the

crystal momentum  $\vec{k}$ , and  $a_{\vec{k}}$  is so chosen that  $\chi_{\vec{k}}$  for each  $\vec{k}$  is orthogonal to the core wave function. The function  $\chi_{\vec{k}}$ , as written, is not normalized. Brown<sup>5</sup> also used this approach for calculating structure factors for Be, and Chaddah and Sahni<sup>19</sup> calculated Compton profiles for a single OPW but included correlation effects in an approximate way and did not assume a spherical Fermi surface (in the extended-zone scheme) as it is done by Brown<sup>5</sup> and by us.

Next we employ the so-called "renormalized-free-atom" (RFA) model.<sup>20</sup> The construction of the crystal wave function has been outlined in the Appendix. The model was successful in fitting experimental isotropic Compton profiles for the first-row transition metals.<sup>21</sup> It has been observed that the RFA wave function gave a good value for the valence charge density at the nucleus for beryllium metal.<sup>22</sup> As for the OPW model we assume a spherical Fermi surface. Whereas the anisotropy in the Compton profiles of beryllium mainly is determined by the Fermi-surface shape,<sup>4</sup> the isotropic profile is not expected to be very sensitive to the detailed shape which is also an assumption that must be inherent in the work on transition metals by Berggren *et al.*,<sup>21</sup> and which must be more serious for those materials.

The results for the valence-electron form factors are shown in Fig. 8. It should be stressed that these curves only have a physical meaning for  $\sin\theta/\lambda$  values corresponding to reciprocal-lattice vectors, and that the behavior between these points depends on the way an atomic fragment has been defined. Nevertheless, for  $\sin\theta/\lambda \geq 0.3 \text{ \AA}^{-1}$  the reciprocal-lattice-vector lengths are so closely spaced that for all practical purposes we may consider the curves as continuous. In the present case, the atomic fragment is defined as the total electron density

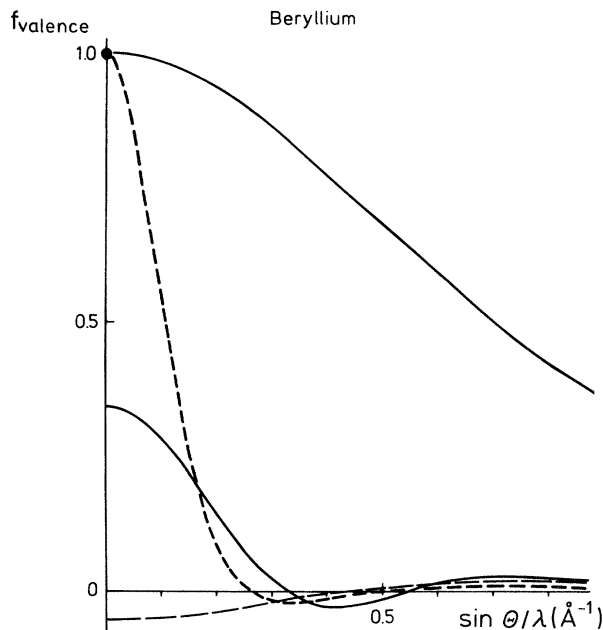


FIG. 8. Beryllium form factors (normalized) starting from 1.0 as follows: free-atom core (HF) (—), and free-atom valence (HF) (---); starting from 0.34 as follows: RFA model (—); and starting from  $-0.06$  as follows: OPW model (---).

within the Wigner-Seitz sphere minus a constant equal to the density at the Wigner-Seitz sphere boundary. This definition leads to values of the form factor different from one for zero-momentum transfer. The OPW model results in form factors lying below the free atom for the lowest-order reflections (the range  $0.25 \leq \sin\theta/\lambda \leq 0.33 \text{ \AA}^{-1}$ ), whereas the RFA model gives values above those of the free-atom model (Fig. 9). The differences between these two simple models at high  $\sin\theta/\lambda$  values (larger than about  $0.5 \text{ \AA}^{-1}$ ) arise from the core orthogonalization. The degree of this deviation is simply proportional to the difference of the overlap of the ansatz valence and the core wave functions.

The isotropic valence-electron Compton profiles calculated from the two models are very similar. The peak values are 1.35 and 1.38 for the RFA and the OPW models, respectively, and for low momenta in quite good agreement with experiment. The general shape is very close to the free, noninteracting electron gas, except for the tail at high momenta. For the OPW calculation, the

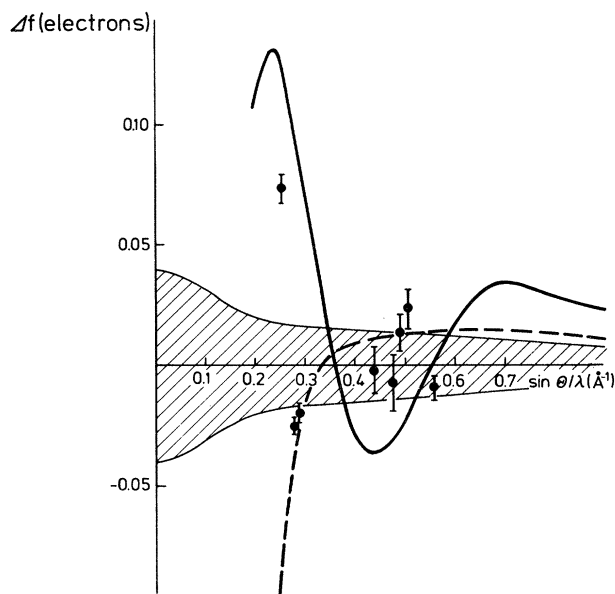


FIG. 9. Deviation of model form factors from the free-atom HF form factor as follows: RFA model (—) and OPW model (---). Hatched area shows  $\pm 1\%$  of the free-atom form factor. Also shown is the present experimental values,  $\bullet$ .

high-momentum tail in the Compton profile is purely an effect of the core orthogonalization. In the RFA model the shape of the atomic ansatz function without core orthogonalization also results in a contribution at high momenta. Nevertheless, also for this model, the major contribution at high momenta arises from core orthogonalization (see Table III).

In Fig. 10 we have shown the results for the isotropic valence Compton profiles together with the valence Compton profiles for the free atom, the noninteracting electron gas, the LCAO calculation,<sup>11</sup> and from the experiment by Maninen and Suortti.<sup>3</sup>

The LCAO calculation by Dovesi *et al.*<sup>11</sup> produces an isotropic Compton profile which is close to the measurement by Manninen and Suortti.<sup>3</sup> The peak value predicted by the theory is slightly too low, and also for high momenta, the theory gives lower values ( $q \geq 1.0 \text{ a.u.}$ ) than the experiment. The disagreement may in part be due to an incomplete correction of the experimental data for resolution smearing, but electron-electron correlation which is not taken into account in the theory, is expected to give rise to an effect of about the right order of magnitude.<sup>23</sup>

TABLE III. Values of the isotropic Compton profile calculated from different simple models. Fermi momentum for the noninteracting free-electron gas is  $p_F = 1.027 \text{ a.u.}$  momentum.

$q$ (a.u.)	Noninteracting electron gas	RFA, no core-orthogonality constraint	OPW	RFA
0	1.459	1.443	1.383	1.354
1.03	0.000	0.008	0.026	0.027
2.00	0.000	0.005	0.018	0.025

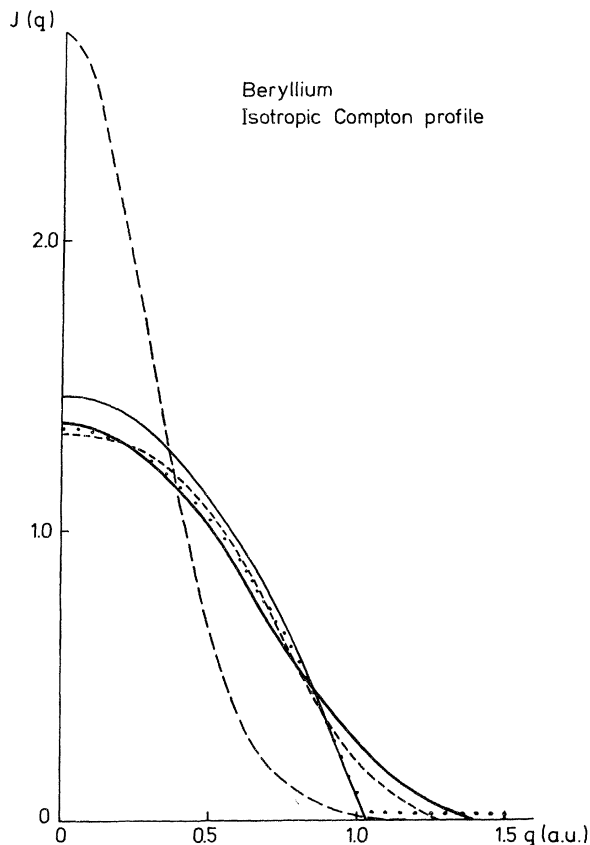


FIG. 10. Isotropic Compton profiles for beryllium as follows: experimental, Manninen and Suortti (Ref. 3) (—); HF atom (---); noninteracting electron gas (—); RFA model (···); and HF LCAO calculation, Dovesi *et al.* (Ref. 11) (----).

## VI. CONCLUSION

We have described the  $\gamma$ -diffraction measurements of eight structure factors for low-order reflections in beryllium. They are believed to be on an absolute scale and without any considerable amount of extinction, although the rocking curves indicate that the samples consist of a few rather perfect regions. The values of the  $\gamma$  structure factors coincide quite well with other recent accurate data sets,<sup>1,6</sup> but are significantly different from the beryllium structure factors measured by Brown.<sup>5</sup>

Matthai *et al.*<sup>24</sup> constructed Wannier functions for beryllium assuming an  $sp_z$  hybridization of the atoms. They find a qualitatively satisfactory agreement with Brown's x-ray data except for the (100) reflection. Since their choice of model was influenced by the conclusions drawn from the analysis of Brown's experimental data, their results cannot be used as a confirmation of the reliability of these data. What nevertheless is in reasonable agreement with Brown's data, is a calculation of structure factors by Becker<sup>25</sup> using linear-response theory. It should be borne in mind that such an approach is based on a series of approximations which may not be valid for systems which deviate strongly from a free-electron-like system as in Be.

The theoretical calculations by Dovesi *et al.*<sup>11</sup> are in reasonable agreement, not only with the present diffraction data, but also with experimental isotropic Compton profiles for beryllium metal. The discrepancies in the Compton profile anisotropies are probably due to errors in the Fermi-surface shape obtained from this theory, whereas the small disagreement in the isotropic profiles may be caused by the neglect of electron-electron correlation effects in the theory. Owing to the relatively good agreement with experiment, the theory by Dovesi *et al.* may be used as a starting point for an understanding of the bonding mechanism in beryllium metal. The density of states calculated by Dovesi *et al.* shows a very large  $p$ -orbital contribution, but the different  $p$  orbitals contribute about the same to the density of states below the Fermi energy, so that at this level the discussion does not clarify why beryllium does not form an ideally hexagonal-close-packed structure and why many of its properties are not isotropic.

The APW calculation by Redinger *et al.*<sup>10</sup> gives structure factors in as close an agreement with experiment as the HF calculation by Dovesi *et al.* Nevertheless, neither of the theories is satisfactory when judged based on the experimental accuracy. It is an open question as to what causes the differences. The results of the HF calculation may be affected by basis-set deficiencies, and by neglect of electron-electron correlation. For the APW calculation (the method has no basis-set problem) the muffin-tin approximation to the potential may be too restrictive. A more advanced treatment of exchange-correlation effects, at least more advanced than the local-density approximation, may be necessary.<sup>26</sup>

The first reaction to the experimental structure factors and Compton profiles was that the latter looked very similar to what one would expect for an almost-free-electron gas, whereas the former were very close to free-atom scattering factors. The more realistic RFA model, however, predicted the right trends for both experiments in spite of its simplicity. It is interesting to note that the OPW and RFA models result in almost identical isotropic Compton profiles, whereas there are definite differences for the low-order structure factors. It may be taken to imply that for such simple structures the Compton profiles are more sensitive to the constraints that the structure puts on the wave function combined with Fermi-surface shape. In terms of the simple models, the Compton profiles depend weakly on  $u(\vec{r})$  which represents the average behavior of the valence-electron wave functions (see the Appendix). The structure factors on the other hand depend solely and sensitively on the function  $u(\vec{r})$ , and seem to emphasize an atomiclike picture in the present case. These arguments should not be pushed further since we have only considered the coarse features in the observables.

## ACKNOWLEDGMENTS

The authors would like to thank Dr. J. Redinger and Mr. G. E. W. Bauer for many useful discussions. The financial support by Die Deutsche Forschungsgemeinschaft and the Danish Natural Sciences Research Council is gratefully acknowledged.



## APPENDIX

In the following we shall give a short outline of how the structure factors and the Compton profiles are calculated from the RFA model. The OPW calculation is also contained in this formalism.

The starting point for the RFA model is a free-atom  $s$  orbital,

$$\chi_s(r) = \frac{1}{\sqrt{4\pi}} R(r),$$

where  $R(r)$  is a radial function. This function is then chopped off at the boundary of the atomic Wigner-Seitz cell which in the actual calculations is replaced by a sphere with the same volume and renormalized as follows:

$$R_{\text{RFA}}(r) = \alpha R(r) \text{ for } r \leq R_{\text{WS}}, \text{ otherwise zero,}$$

where  $\alpha$  is a constant chosen so that

$$\int_0^{R_{\text{WS}}} R_{\text{RFA}}(r)^2 r^2 dr = 1$$

( $R_{\text{WS}}$  is the radius of the "Wigner-Seitz sphere"). These functions are then repeated around each atom, thus resulting in a periodic function,

$$u(\vec{r}) = \sum_{\text{atoms}} R_{\text{RFA}}(\vec{r} - \vec{r}_{\text{atom}}),$$

and the crystal wave functions are given as

$$\psi_{\vec{k}}(\vec{r}) = u(\vec{r}) e^{i\vec{k} \cdot \vec{r}},$$

where the extended-zone scheme is employed.

The charge density  $\rho_v$  corresponding to these wave functions is given by

$$\rho_v(\vec{r}) = n_e |u(\vec{r})|^2,$$

with  $n_e$  being the number of valence electrons per unit cell (for Be,  $n_e = 4$ ). The corresponding structure factor  $F(\vec{h})$  is the Fourier transform of  $\rho_v$  which is most easily calculated by first calculating the form factor for an atomic fragment equal to the density within the Wigner-Seitz sphere minus a constant equal to the density at the surface of this sphere,

$$f_{\text{RFA}} \left[ \frac{\sin\theta}{\lambda} \right] = \int_0^{R_{\text{WS}}} \{ [R_{\text{RFA}}(r)]^2 - [R_{\text{RFA}}(R_{\text{WS}})]^2 \} \\ \times \frac{\sin(4\pi r \sin\theta/\lambda)}{4\pi r \sin\theta/\lambda} r^2 dr,$$

and next the structure factor through

$$F(\vec{h}) = 2f_{\text{RFA}} \left[ \frac{h}{2} \right] \cos \left[ 2\pi \left[ \frac{h-k}{3} + \frac{1}{4} \right] \right].$$

This does not include the effect of thermal vibrations.

The momentum density  $\rho_v(\vec{p})$  is obtained from the crystal wave functions by first Fourier-transforming these and subsequently squaring and summing over occupied  $\vec{k}$

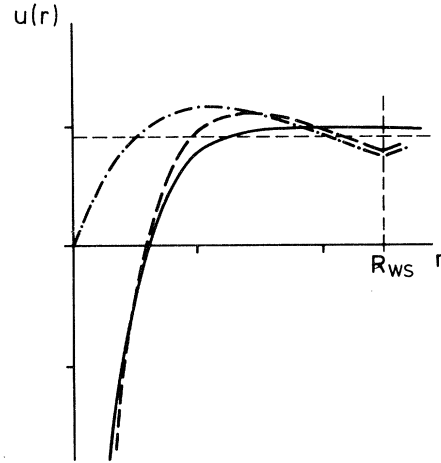


FIG. 11. RFA and OPW wave functions and periodic part of Block function as follows: OPW model (—); RFA, (---) single Slater-atom orbital without core-orthogonality constraint; and RFA, valence orbital orthogonal to the atomic core orbitals (— · —).

states in the extended-zone scheme. The approximation that the periodic part of the crystal wave function is independent of the crystal momentum  $\vec{k}$  has the consequence that the momentum density is a step function. The isotropic Compton profile is then calculated by

$$J(q) = 2 \int_q^\infty p \langle \rho_v(p) \rangle dp,$$

where  $\langle \rangle$  denotes spherical averaging. The details of the calculation have been described thoroughly for the hexagonal-close-packed structures by Berggren, Manninen, and Paakkari.<sup>27</sup>

In the RFA calculations presented here, we have used Slater-orbital representation with the screening constants by Clementi and Raimondi,<sup>28</sup> i.e.,

$$\chi_{1s}(r) \sim \exp(-3.6848r),$$

$$\chi_{2s}(r) \sim r \exp(0.9560r) - a\chi_{1s}(r),$$

where "r" is in units of Bohr radii, and a constant  $a$  is chosen to make the  $2s$  orbital  $\chi_{2s}$  orthogonal to the core orbital,  $\chi_{1s}$ . We calculate only the contribution from the  $2s$  orbital to the Compton profile since the  $1s$  orbital is hardly affected by the crystal environment.<sup>29</sup>

The OPW results are simulated by the same procedure; we are only starting from an atomic  $1s$  orbital for the core and a  $1s$ -like function for the valence, but very diffuse, so that it is almost constant within the Wigner-Seitz cell.

In Fig. 11 the periodic part  $u$  of the wave functions from the RFA model, with and without core orthogonalization, as well as the plane-wave and OPW models, have been shown.

- \*Present address: Laboratoire de Minéralogie et Cristallographie, Université de Nancy I, Boîte Postale 239, F-54506 Vandoeuvre-les-Nancy, France.
- <sup>1</sup>F. K. Larsen and N. K. Hansen, *Acta Crystallogr. A* (in press).
- <sup>2</sup>F. K. Larsen, M. S. Lehmann, and M. Merisalo, *Acta Crystallogr. Sect. A* **36**, 159 (1980).
- <sup>3</sup>S. Manninen and P. Suortti, *Philos. Mag. B* **40**, 199 (1979).
- <sup>4</sup>N. K. Hansen, P. Pattison, and J. R. Schneider, *Z. Phys. B* **35**, 215 (1979).
- <sup>5</sup>P. J. Brown, *Philos. Mag.* **26**, 1377 (1972).
- <sup>6</sup>P. Suortti, *Acta Crystallogr. Sect. A* **38**, 648 (1982).
- <sup>7</sup>R. F. Stewart, *Acta Crystallogr. Sect. A* **33**, 33 (1977).
- <sup>8</sup>Y. W. Yang and P. Coppens, *Acta Crystallogr. Sect. A* **34**, 61 (1978).
- <sup>9</sup>S. T. Inoue and J. Yamashita, *J. Phys. Soc. Jpn.* **35**, 677 (1973).
- <sup>10</sup>J. Redinger, G. E. W. Bauer, and N. K. Hansen (unpublished).
- <sup>11</sup>R. Dovesi, C. Pisani, F. Ricca, and C. Roetti, *Phys. Rev. B* **25**, 3731 (1982); R. Dovesi, L. Pisani, R. Ricca, and C. Roetti, *Z. Phys. B* **47**, 19 (1982).
- <sup>12</sup>J. R. Schneider, P. Pattison, and H. A. Graf, *Nucl. Instrum. Methods* **116**, 1 (1979).
- <sup>13</sup>D. R. Chipman, *Acta Crystallogr. Sect. A* **25**, 209 (1969).
- <sup>14</sup>J. R. Schneider, *Acta Crystallogr. Sect. A* **33**, 235 (1977).
- <sup>15</sup>P. J. E. Aldred and M. Hart, *Proc. R. Soc. London, Ser. A* **332**, 239 (1973).
- <sup>16</sup>J. R. Schneider, *J. Appl. Crystallogr.* **8**, 530 (1975).
- <sup>17</sup>P. A. Doyle and P. S. Turner, *Acta Crystallogr. Sect. A* **24**, 390 (1968).
- <sup>18</sup>R. Benesch and V. H. Smith, Jr., *Phys. Rev. A* **5**, 114 (1972).
- <sup>19</sup>P. Chaddah and V. C. Sahni, *Phys. Lett.* **56A**, 323 (1976).
- <sup>20</sup>L. Hodges, R. E. Watson, and H. Ehrenreich, *Phys. Rev. B* **5**, 3953 (1972).
- <sup>21</sup>K. F. Berggren, S. Manninen, T. Paakkari, O. Aikala, and K. Mansikka, in *Compton Scattering*, edited by B. Williams (McGraw-Hill, New York, 1977), pp. 153–159.
- <sup>22</sup>B. Koiller and L. M. Fallicov, *Phys. Rev. B* **12**, 2080 (1975).
- <sup>23</sup>G. E. W. Bauer and J. R. Schneider, *Solid State Commun.* **47**, 673 (1983).
- <sup>24</sup>C. C. Matthai, P. J. Grout, and N. H. March, *J. Phys. F* **10**, 1621 (1980).
- <sup>25</sup>*Electron Distributions and the Chemical Bond*, edited by P. Coppens and M. B. Hall (Plenum, New York, 1982), pp. 153–172.
- <sup>26</sup>M. Y. Chou, P. K. Lam, and M. L. Cohen [*Solid State Commun.* **42**, 861 (1982)] performed *ab initio* calculations of the static structural properties of Be by solving the Kohn-Sham equations using the self-consistent pseudopotential method. They also employed the local-density approximation and the Hedin-Lundqvist expression for the exchange-correlation potential. Recently Chou *et al.* [*Phys. Rev. Lett.* **49**, 1453 (1982)] extended these pseudopotential calculations to determine directional Compton profiles of Be and found good agreement with experiment once electron-electron correlation is taken into account. Chou (private communication) also calculated structure factors and the valence density of Be. The first four structure factors agree to within ~0.5% with the  $\gamma$ -ray data and the valence density is in good agreement with the experimental valence-density maps calculated by Larsen and Hansen.<sup>1</sup> We therefore conclude that the main problem with the presently available APW calculations on Be should be caused by the muffin-tin approximation to the crystal potential.
- <sup>27</sup>K. F. Berggren, S. Manninen, and T. Paakkari, *Phys. Rev. B* **8**, 2516 (1973).
- <sup>28</sup>E. Clementi and D. L. Raimondi, *J. Chem. Phys.* **38**, 2686 (1963).
- <sup>29</sup>R. Dovesi, G. Angonoa, and M. Causa, *Philos. Mag. B* **45**, 601 (1982).